PHILOSOPHICAL TRANSACTIONS OF THE ROYAL SOCIETY A MATHEMATICAL, PHYSICAL & ENGINEERING SCIENCES

Extended ionic models from *ab initio* calculations

Mark Wilson

Phil. Trans. R. Soc. Lond. A 2000 **358**, 399-418
doi: 10.1098/rsta.2000.0538

THE ROYAL SOCIETY

Extended ionic models from *ab initio* calculations

By Mark Wilson

Physical and Theoretical Chemistry Laboratory, University of Oxford, South Parks Road, Oxford OX1 3QZ, UK

The atomistic computer simulation of ionic materials has undergone massive changes over the last three decades. Major developments will be reviewed, and possible future directions explored. *Extended* ionic models account for an ion's response to the environment (for example, polarization or a change in size and shape) and introduce a *many-body* character. The exploration of the applicability of such models, which exclude such effects as charge transfer and chemical bond formation, is practical as large-scale simulations remain possible. High-level *ab initio* electronic structure calculations, which form a source of parameters in which each *aspect* of the model is parametrized *independently*, will be highlighted. The unambiguous nature of the resulting parameter sets will be demonstrated by simulating a range of very different, but linked, systems. Possible future directions will be explored.

Keywords: ionic model; molecular dynamics; polarization; transferability; electronic structure calculations

1. Introduction

The construction of models to understand the structure and dynamics of materials at an atomistic level is nothing new. Simple sphere-packing models have been used for many years. More complex materials, in which the most useful simple repeating structural motif is a local coordination polyhedron, have also been extensively studied, using simple ball and stick models. The motivation behind the construction of such models stems from the fact that, away from the local ordering (the short-range order, SRO), the geometrical relationships between atoms, even in the simplest close-packed systems, become extremely complex. This complexity is greatly increased for systems in which many-body forces (leading to bond directionality) become significant.

The construction of relatively simple models of this type lends itself naturally to the use of computers (Allen & Tildesley 1987, 1993). In the simplest cases, models can be constructed by applying the same sorts of arguments used to generate the physical models, either by packing spheres of a certain size together or by linking local polyhedra in some prescribed manner. In such models, no interaction potentials are assumed between species, with successive configurations being generated by applying the same building procedure; no dynamical information regarding the systems is obtained. An alternative approach is to move away from the concept of hard spheres or rigid local polyhedra and assume a continuous (pairwise additive) interaction

energy function acting between species. In the simplest cases for noble-gas closed-shell atoms, the broad system properties can be reproduced by decomposing the energy of interaction between each pair of atoms into attractive (dispersive) and repulsive terms (a Lennard–Jones potential).

At the simplest level (the rigid-ion model, RIM), ionic systems can be modelled using the same type of simple pair-potential formalism, for example, via a Born–Mayer potential (see, for example, Sangster & Dixon 1976; Woodcock & Singer 1971) of the type

$$U^{\mathrm{BM}}(r_{ij}) = \frac{Q^i Q^j}{r_{ij}} + B^{ij}\exp(-\alpha_{ij} r_{ij}) - \sum_{n=6,8,\ldots} \frac{C_n}{r_{ij}^n} f_n(r_{ij}), \tag{1.1}$$

where $Q^{i(j)}$ is the charge on ion $i(j)$, B^{ij} and α_{ij} are the short-range repulsion parameters, and C_n and f_n are the dispersion coefficients and damping functions, respectively. In these cases, a system that is 'ionic' is one whose properties are reproduced by an interaction model based upon discrete closed-shell ions with integer charges. However, the domain of applicability of this simplest ionic model is severely restricted. While the structural properties of simple systems, such as the alkali halides, are well reproduced, this model fails to account even for the static crystal structure of a system like $MgCl_2$, despite the large electronegativity difference between the elements involved, which would lead one to believe that an ionic description was in order. In the liquid state, such models fail to reproduce the so-called first sharp diffraction peak (FSDP) (Enderby & Barnes 1990), a low scattering angle feature on the static structure factor that corresponds to ordering, in the metal cation sublattice, on an intermediate (5–10 Å) length-scale (Woodcock *et al.* 1976; Elliott 1990, 1991). The failure to predict even the static structure has traditionally rendered the modelling of the wealth of interesting dynamics impossible (Enderby & Barnes 1990).

The answer lies in the fact that the ions need not be simple charged hard-spheres. In an 'extended' ionic model, they may undergo polarization (induction) and may undergo changes of size and shape ('compression' and 'deformation') due to the interactions with their neighbours. Explicit charge transfer or chemical bond formation is, however, always excluded.

Here, we are interested in the *extended* ionic model, which allows for *the changes in an ion's properties that are caused by changes in its environment*, and, hence, incorporate a many-body character in the interactions. We will show how they may account for many departures from the predictions of the simple ionic model that are conventionally attributed to 'covalency'.

The reason that the use of an extended ionic model is practical is essentially twofold. Firstly, it may be used as the basis of tractable computer simulation methods, which permit the study of large systems for long times. Secondly, and more fundamentally, because it is based upon the properties of individual ions, the ionic model is (or should be) *transferable*: it may be used on different phases of the same material, on mixtures, and, furthermore, the interaction model for one material should be recognizably related to that of a chemically similar one by a change in ion size or similar property. A transferable model may be tested on one phase and used on another, tested in the bulk and used for a surface, etc. Because of the relationship between materials, the origin of structural trends may be understood, and a first guess at an interaction model for one material may be constructed from an established model for another. Born–Haber cycles may be constructed to analyse energetics.

The traditional methods for handling such many-body forces has been the shell model (Dick & Overhauser 1958) or the breathing-shell modifications (Schröder 1966), in which the polarization of the ion is represented in a particular mechanical way by means of a charged shell connected to a charged core by a harmonic spring of force constant k. The effect is to minimize the number of parameters required to fully describe the model, allowing for parametrizations from a minimal (experimental) dataset. However, this strategy reduces the flexibility available to accurately reproduce the many-body effects, a limitation that becomes clear when comparing with the results of electronic structure calculations of *ionic* properties (such as induced dipoles) (Madden & Wilson 1996). Additionally, interactions between like species (in particular the anion–anion interactions) are relatively uncontrolled, and so systems with an excess of anions may be harder to model.

An alternative approach, used in the polarizable-ion model (PIM) (following the work of Sprik (1991*a*, *b*), Sprik & Klein (1988) and Sprik *et al.* (1990)) uses point dipoles whose dynamical motion is incorporated into the model via an extended Lagrangian formalism (Madden & Wilson 1996). Equations of motion can then be generated to account for the time evolution of the induced moments, and these can be integrated in parallel with the ionic equations of motion in a classical analogue of the Car–Parrinello method (Car & Parrinello 1985). Non-coulombic (short-range) interactions with the dipoles are also included in a physically transparent manner. As a result, the input parameters (the ion polarizabilities and a parameter controlling the short-range effects) are much more transferable than the shell charge and spring constant used in the traditional shell model. Additionally, this method allows for the inclusion of higher-order moments (quadrupoles and octupoles) (Wilson *et al.* 1996*a*, *b*; Wilson & Madden 1997*a*), which are difficult to incorporate within the mechanical representation of the physics afforded by the shell model. Ion deformation effects can be included both at a spherical relaxation ('breathing') level (the compressible-ion mode, CIM) or at a more general deformation level (the anisotropic-ion mode, AIM). Again, the latter can include distortions up to, and including, quadrupoles (Rowley *et al.* 1998, 1999). Similar effects have been included in other models, such as the potential-induced breathing (PIB) model and models based on the electron gas (Boyer *et al.* 1985; Lacks & Gordon 1993), which allow for the breathing of the anions calculated using a Watson sphere.

A central reason for wishing to pursue a model of this type is that, if the representation of the system as a collection of closed-shell ions holds, then well-directed *ab initio* calculations should be practicable, which allow for the unambiguous determination of the physically transparent parameters (Lewis & Catlow 1985). It is worth noting, at this point, that the *ab initio* calculations of the type proposed cannot (within current computer power) be used to model the systems of interest on the length-scales and time-scales required. Furthermore, techniques based on density-functional methods do not lend themselves well to modelling systems of closed-shell species.

2. Parametrization

(*a*) *History*

The long-standing difficulty with examining the applicability of the ionic model (including the many-body effects) is that the *individual* ion properties that determine

the interionic interactions in condensed phases cannot be determined from experimental data alone without further assumptions (Harding 1990). In the basic-shell (or breathing-shell) models, the problem is controlled by imposing a particular mechanical representation of the many-body effects (the charged shell connected to a charged core by a harmonic spring).

(*b*) *Using ab initio sources*

Modern computational techniques allow for small-scale electronic structure calculations in order to determine the properties of single ions within their condensed phase environment. This breaks the above impasse and allows an ionic model to be parametrized unequivocally. Recently it has been shown how interaction models that allow for an accurate representation of the many-body effects uncovered by such calculations may be constructed and used in tractable computer simulation schemes (Madden & Wilson 1996).

Calculations can be divided into two broad categories. 'Direct' methods are designed specifically for parametrizations, focusing upon the ion properties of interest. 'Indirect' methods are calculations that contain important information regarding the system but require additional knowledge or approximations in order to extract parameters. A distinction is drawn at this point, as, although direct calculations are clearly desirable from the point of view of wishing to construct potential models, they are not always practicable.

(i) *Direct methods*

The central parameters in controlling the polarization aspects of the ionic model are the Born–Mayer terms, the polarizabilities and damping parameters, the latter controlling the effect of short-range overlap interaction on the induced moments (Madden & Wilson 1996).

Polarizabilities The variation of the mean polarizability, α, of an in-crystal anion with lattice parameter R has been calculated at various levels of representation of the crystalline environment (CRYS and CLUS) and at two levels of *ab initio* theory (J̈emmer *et al.* 1998; Domene *et al.* 1999). The CRYS environment is simply that of a lattice of point charges surrounding the anion of interest, whereas the CLUS further includes the effect of the full electron density of the first shell of nearest-neighbour cations. Such calculations can be compared directly with experiment, as the change in refractive index with pressure can be measured directly and related to the change in polarizability with lattice parameter. At the highest level of theory considered (CLUS(MP2)), these results are in excellent agreement with experiment (J̈emmer *et al.* 1998; Domene *et al.* 1999). The curves of polarizability against lattice parameter have a characteristic sigmoid shape, at least for bound ions such as halides.

Short-range repulsion parameters Pyper and co-workers (Pyper 1991; Harding & Pyper 1995) have shown how the short-range repulsive parameters in equation (1.1) can be derived from analogous *ab initio* calculations. Mahan & Subbaswamy (1990) have used similar arguments from within a density-functional framework. In these cases, the self-consistent anion electron density is calculated at a series of lattice

parameters about the equilibrium value. The energy required to place the ion in that site at that density (the rearrangement, or 'self', energy) and the energy of interaction of the anion with the nearest-neighbour cations (the overlap energy) are then obtained. For the simplest pair-potentials, these quantities can simply be combined or the two energies may be kept separate in order to parametrize a full CIM (Wilson *et al.* 1996*c*) in which the internal state of an ion depends on the change δ^i in its radius $\bar{\sigma}^i$, leading to a total short-range (sr) energy given by

$$U^{\mathrm{sr}} = \sum_{j<i} u_{\mathrm{CI}}^{ij}(r^{ij} - (\bar{\sigma}^i + \delta^i) - (\bar{\sigma}^j + \delta^j)) + F(\delta^i), \tag{2.1}$$

where u_{CI}^{ij} is the pair overlap term and $F(\delta^i)$ is the rearrangement energy. At the self-consistent energy minimum for a given set of ion coordinates $\{r^i\}_{i=1,N}$, U^{sr} is minimized to determine the adiabatic ion radii given by $\{\delta^i_{\mathrm{opt}}\}_{i=1,N}$. As with the induced moments, the ion radius is included as an additional degree of freedom, allowing parallel dynamics to be performed.

Induction damping In order to parametrize the effects of damping, the nearest-neighbour cations are distorted in order to generate the required moment on the central anion (Fowler & Madden 1985). For the closed-shell spherical ions implicit in our model, the polarizability tensors reduce to single polarizabilities, α, B and C, the dipole polarizability, dipole–dipole–quadrupole hyperpolarizability, and the quadrupole polarizability, respectively.

In parametrizing the models, the induced dipoles and quadrupoles are written in terms of the pair separations of the ions, and so the moments generated by the short-range interactions are expressed in the same form,

$$\mu_\alpha^{\mathrm{sr},i} = -\alpha^i \sum_{j\neq i} \frac{r_{ij,\alpha}}{r_{ij}^3} f_{ij}(r_{ij}), \tag{2.2}$$

where f_{ij} is a short-ranged function used by Tang & Toennies (1984) (Tang & Toennies are hereafter referred to as TT) to model dispersion damping extended by adding a variable c:

$$f(r_{ij}) = -c \sum_{k=0}^{k_{\max}} \frac{(br_i)^k}{k!} \mathrm{e}^{-br_{ij}}. \tag{2.3}$$

The parameter b is referred to as the short-range damping parameter (SRDP). The c parameter is added as, although the effect of the short-range interactions on the moments is referred to throughout as a damping, it is possible for the magnitude of the short-range moment to exceed the asymptotic moment (Fowler & Madden 1985). The original TT function is not flexible enough to model this behaviour.

Figure 1*a*, *b* shows the variation of the dipoles and quadrupoles for a series of inward and outward distortions for LiF, NaF and KF (Jemmer *et al.* 1999).

Figure 1*b* clearly shows the reversal of sign of the total moment with respect to the asymptotic. Given this, it is also clear that figure 1*a* shows the same general behaviour but with a minimum in the curve corresponding to a much larger inward displacement.

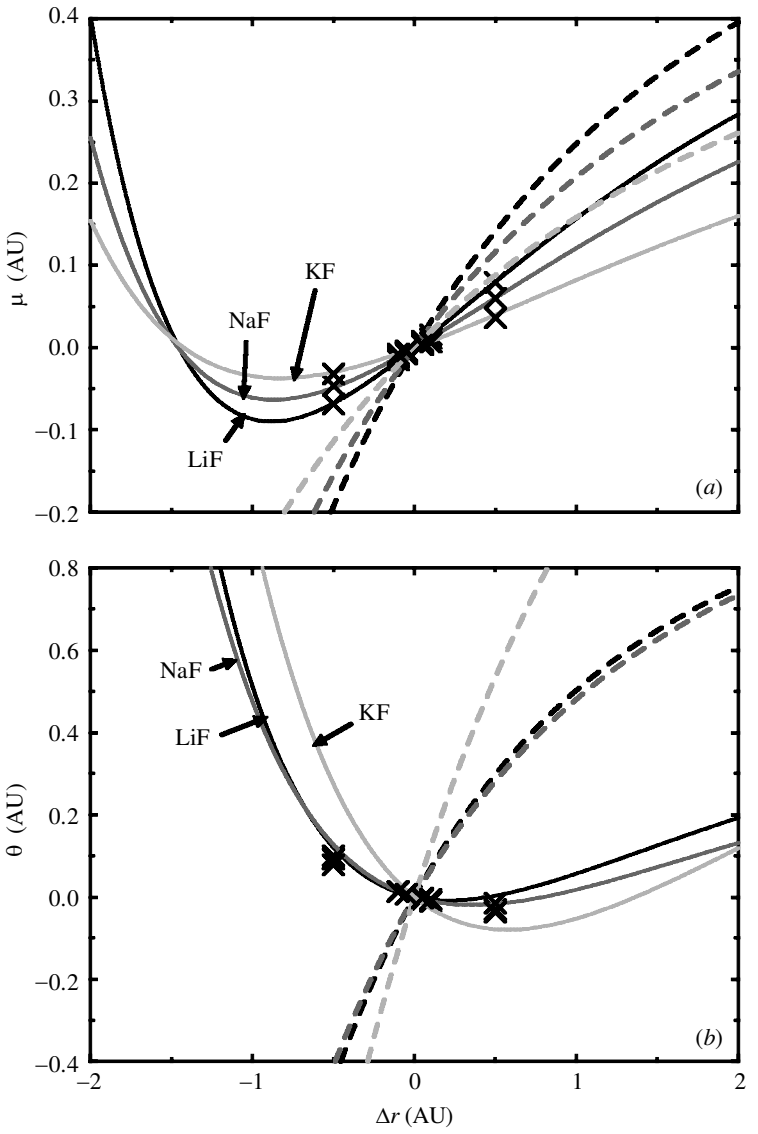

Figure 1. (*a*) Variation of the total induced dipole on a central anion surrounded by a nearest-neighbour shell of cations embedded in a point charge lattice as a cation is moved away from the anion. A positive displacement corresponds to an outward movement. The crosses represent the *ab initio* points, the solid lines the fits/scaled curves (see text for details), and the dotted lines the asymptotic moments induced from the movement of the charges only (Jemmer *et al.* 1999). (*b*) As (*a*) except for the induced quadrupoles. Note how the total predicted moment has the opposite sign to the asymptotic. The dotted lines are ordered as the solid.

(ii) *Indirect*

An alternative to the above procedures is to use less direct calculations to parametrize models. For example, a common *ab initio* technique is to perform *total* energy calculations on periodic systems or isolated clusters, at a series of configurations,

which can then be used as input to fit an *assumed* energy function (for example, equation (1.1)). The drawback of this approach is that the assumed energy function must contain all of the appropriate physics in order to produce a truly transferable model. For example, 'polarization effects' can appear as enhanced (non-physical) cation–cation dispersion terms in equation (1.1) (Kumta *et al.* 1988; Gale *et al.* 1992).

However, although such calculations do not contain enough information to parametrize an entire model from scratch unambiguously, they are very useful in the limit of already having a significant section of the model well-defined.

(*c*) *Other parametrization techniques*

If high-level calculations are not available or practicable, other sources must be tapped to complete parameter sets. Specific experimental information can be very useful for filling in missing terms in potential models. In the alkaline-earth oxides, for example, the parameters governing the ion deformability can be derived by looking at specific phonons in which the relative motion of the anion and cation sublattices is well understood. This allows specific dipole-only and quadrupole-only modes to be isolated and used to parametrize those terms independently (Rowley *et al.* 1998, 1999).

An alternative to using experimental information to focus on specific missing model elements is to derive new potential parameters using (hopefully) simple scaling procedures. Thus, if a parameter set is known for one system, it may be possible to transfer the parameters to another system in a physically transparent manner, for example, by scaling in terms of ion radii.

In order to demonstrate the use of scaling procedures, we shall consider the three sets of *ab initio* calculations.

Short-range parameters The simple Born–Mayer potential parameters should scale with the ion radii (see, for example, Sangster & Dixon 1976; Woodcock & Singer 1971), such that

$$B_{ij} = A_{ij} \exp[\alpha(\sigma_i + \sigma_j)], \tag{2.4}$$

where $\sigma_{i(j)}$ is the radius of ion $i(j)$, and A_{ij} is a constant.

A more complex question of parameter scaling concerns the CIM and AIM parameters. Clearly, since cation radii are still inherent in the short-range energy functions, then one would hope that the parameters may transfer in the same manner as for the Born–Mayer pair-potential terms for the overlap terms. The rearrangement term, however, may ideally become a property of the anion only, and, hence, will be independent of the cation behaviour. Indeed, work on the alkaline-earth oxides shows that this is the case (Wilson *et al.* 1996*a*, *b*; Wilson & Madden 1997*a*). Furthermore, the potential parameters may be transferred *inter*-stoichiometrically (Wilson & Madden 1997*b*; Rowley *et al.* 1998, 1999). The latter is a particularly significant observation as it allows parameters to be defined for systems difficult to attack with the prescribed *ab initio* methods. For systems of stoichiometry M_2X_3, for example, the crystal structures are of relatively low symmetry with correspondingly large unit cells. As a result, the simple distortions described previously are not practicable.

Polarizabilities Recent work has focused on the dependence of the anion polarizability on lattice parameter (Jemmer *et al.* 1998; Domene *et al.* 1999). Most interestingly, one can show how these curves for different systems are simply related by scaling in terms of both the relative cation sizes and the free ion polarizabilities. The important implication of this scaling procedure is that complete curves can be generated for a given system from a relatively small dataset. As a result, curves for cations such as Rb^+ and Cs^+ may be generated, despite the fact that these cations contain too many electrons for computationally tractable *ab initio* calculations.

Induction damping As with the short-range repulsion parameters, it is clear that the SRDPs *should* scale in some way with ion radii. Ideally, one would be able to write

$$b = d/(\sigma_+ + \sigma_-), \tag{2.5}$$

where d is a property of a particular anion. Additionally, if the spirit of the original TT dispersion damping functions still holds, then one might be able to use the *same* SRDPs for the short-range dipoles and quadrupoles for a given system simply by increasing $k_{\max}$ in equation (2.3).

Figure 1*a*, *b* shows the calculated dipole and quadrupole moments for the three chlorides, LiCl, NaCl and KCl, along with the curves corresponding to the TT function fits (Jemmer *et al.* 1999). Also shown in the figure are the asymptotic moments corresponding to each distortion. In figure 1*a*, only the LiF *ab initio* points have been used to fit the TT function. The other two curves, for NaF and KF, have been obtained by varying only the b parameter, while keeping both c and $k_{\max}$ constant in equation (2.3). The excellent correspondence between these scaled curves and the *ab initio* calculations indicates that the general scaling procedures outlined are valid. Furthermore, the *same* parameters transfer to both the fluorides and LiBr (Jemmer *et al.* 1999), indicating that this dipole curve may be universal for the halide systems.

In figure 1*b*, the curves are as predicted from the scaling procedures by keeping both b and c constant but changing $k_{\max}$ from 4 to 6, in the spirit of the original TT functions used to model dispersion damping. The agreement between these scaled curves and the calculated points is very good considering the relative rigidity of the scaling argument we have imposed. Furthermore, it is clear that the presence of a minimum in these curves, corresponding to inward distortions, is a real general system property.

Figure 1 points towards the existence of a universal curve for the induced moments, analogous to that obtained for the variation of the ion polarizability with lattice parameter. Increased computer power will allow for more complete calculations in order to confirm these predictions.

3. Problem solving

Having established clear routes for developing pair-potentials, we shall now move on to highlight how such potentials may be used to simulate a wide range of systems and system properties. In order to highlight how these methods are applicable, we choose to divide problems into different classes of length-scale, time-scale and system complexity (more than two species).

(*a*) *Overview*

An important current aspect in the analysis of computer simulation results lies in the reduction of the information afforded to a manageable level. This problem will be particularly acute in disordered systems that lack any spatial repetition. Relatively simple structural probes, such as radial distribution functions (RDFs), structure factors and bond-angle distributions (BADs), are relatively insensitive.

A possible method of characterizing the spatial arrangement of the ions is via a Voronoi analysis (Naberukhin *et al.* 1991; Bernal 1964; Finney 1970). In a topologically disordered structure, the vertices of the Voronoi polyhedra (VP) define a group of four atoms (the Delauney simplices, DS), about which a circumsphere can be constructed that passes through the four atoms such that no other atom centre lies within that circumsphere. The distribution of circumsphere radii is, therefore, a useful measure of the empty space. Additional information is available from the relative positions of the voids in real and reciprocal space (Naberukhin *et al.* 1991; Bernal 1964; Finney 1970). The void structure can be monitored by treating the DS as radiation scattering particles with positions $\{\mathbf{R}^i\}_{i=1\rightarrow N_V}$:

$$S_{\mathrm{VV}}(k) = \left\langle N_V^{-1} \sum_{i,j=1}^{N_V} \exp(\mathrm{i}\mathbf{k}\cdot\mathbf{R}^{ij}) \right\rangle. \tag{3.1}$$

In liquid $ZnCl_2$, for example, S_{VV} shows two main peaks in the same positions as the FSDP, and the principal peak in S_{ZnZn}, with the FSDP peak by far the most intense. The relatively large intensity of the FSDP in S_{VV} indicates that, as we shall see later, changes in the IRO in this system may be best observed through monitoring the voids rather than the ions themselves. Additionally, the information available from the void structure may be simplified by 'coarse-graining' methods, in which near-neighbour voids are grouped together.

Another popular method for understanding non-local structure is via a ring analysis, which paints a broader picture of how this local connectivity expands onto a longer length-scale. As with the voids, however, the information is less physically transparent than the simple RDFs or BADs. Again, distribution functions can be defined governing the spatial relationship between different ring sizes or rings with voids, etc. Furthermore, distribution functions can be constructed to look at the relationships between voids and rings.

(*b*) *Length-scales*

The size of the simulation cell must be large enough to encompass the significant system length-scales, or else the imposition of the boundary conditions will have significant implications for the system properties.

In this section, we shall use some systems of MX_2 stoichiometry as examples. Figure 2 (inset) shows the circumsphere radius distribution for several MX_2 systems. The $ZnCl_2$ RIM distribution is very similar to the ambient pressure distributions observed for SiO_2, with the larger mean void size reflecting the shorter anion–cation separations in SiO_2. The $ZnCl_2$ PIM distribution has a similar shape to that of the RIM, but is significantly broader, reflecting the greater range of void sizes and suggesting the reduced uniformity of the cation subdensity associated with the formation of the FSDP. The circumsphere radius distribution for $BeCl_2$ is significantly broader

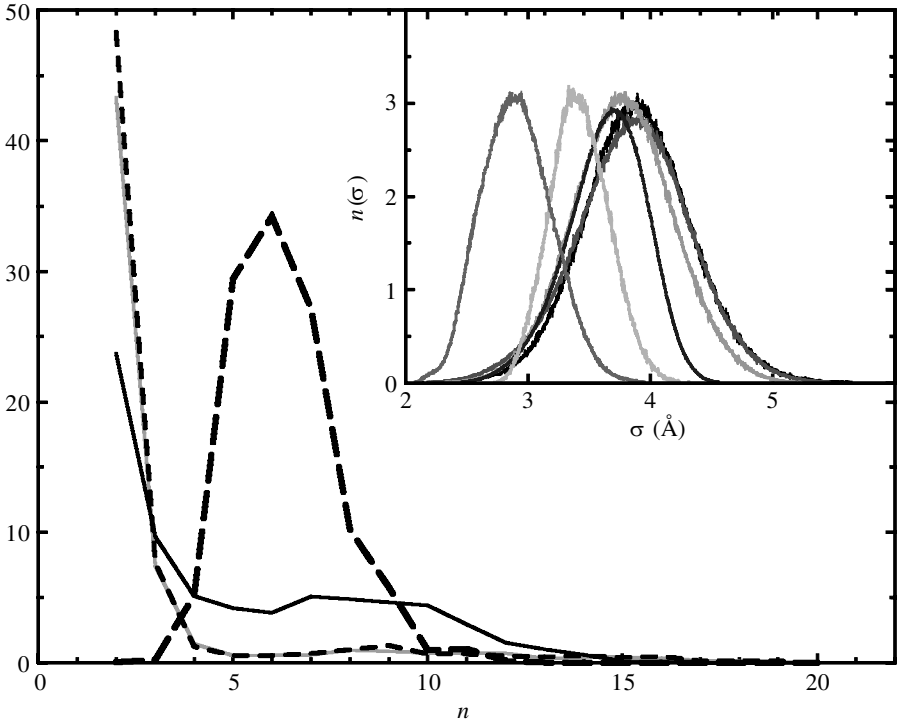

Figure 2. Ring size distributions for SiO_2 (long dashes), $ZnCl_2$ (solid line), cation radius 0.45 Å (light line) and cation radius 0.55 Å (short dashes). The inset shows the circumsphere radii distribution calculated using a Voronoi analysis. Key, from left to right: SiO_2, $ZnCl_2$ RIM, $ZnCl_2$ PIM, $BeCl_2$, cation radius 0.55 Å, cation radius 0.45 Å (see text).

than the $ZnCl_2$ curves characteristic of the chain structure. The beauty of simulation is that one can try to bridge the gap between these two systems by performing a series of simulations for cation sizes intermediate between Be^{2+} and Zn^{2+} (radii of 0.30 and 0.74 Å, respectively). Figure 2 (inset) also shows the circumsphere radius distributions for cations with radii of 0.45 and 0.55 Å.

Figure 2 shows some typical ring-size distributions for a set of MX_2 systems calculated over many picoseconds of dynamics in the liquid state. The ring structure of silica has a peak at $n = 6$ (six Si–O units), indicative of the structure found in the cristobalite polymorph, but also five- and three-membered rings, indicative of the quartz structure (Vashishta *et al.* 1990). In the $ZnCl_2$ PIM, the most abundant rings are two membered, with a secondary peak at between $n = 7$ and $n = 10$, as the anion polarization effects are large enough to be able to stabilize edge-sharing tetrahedral units, at least as structural transients, with the edge-sharing anion–cation pairs forming a single two-membered ring. Such two-membered rings are relatively rigid units and so force a relatively chain-like section of ring, which leads to longer completion pathways.

Both intermediate cation systems are dominated by two-membered rings and show a significant number of rings even larger than those observed for $ZnCl_2$. The increase in the number of two-membered rings is a direct result of the reduction in cation radius with respect to that of Zn^{2+}, in that the M–X–M bond angle has been reduced

yet further. As a result, there are significantly more rings that contain several of the two-membered rings than in $ZnCl_2$, and, as a result of the inherent rigidity of these units, these rings are larger.

This latter result allows us to finalize our interpretation of the void radii distribution in figure 2 (inset). The presence of the larger rings constructed from the relatively rigid two-membered units leads to the presence of larger voids within these rings than are present in $ZnCl_2$. The mean void size falls at the pure $BeCl_2$ 'limit' as the ring structure (beyond simple two-membered species) disappears in favour of the chain structure. The charge-neutral nature of these chains means that they fit together relatively efficiently.

(*c*) *Time-scales*

We have seen above how simulation methods can be used as an aid to understanding the properties of the disordered amorphous systems. In this section, we shall show how a change of state (the crystallization from the liquid state) can be studied and monitored in $ZnCl_2$, which forms a layered crystal structure. As a result, the crystallization event represents a reduction in dimensionality of the system from a three-dimensional disordered network to a pseudo-two-dimensional stack of MX_2 'sandwiches'.

Figure 3 shows a molecular graphics 'snapshot' for a run after *ca.* 1500 ps with 333 $ZnCl_2$ molecules at 600 K having started from a liquid configuration at 700 K. The dynamical formation of this layered structure can be readily followed by looking at the development of specific structure factors, $S_{ZnZn}(k)$. Figure 4 shows the evolution of two structure factors corresponding to the 0–44 and 0–43 directions ($\times 2\pi/L$, where L is the simulation box length, to get the actual k magnitudes), corresponding to 1.15 and 1.01 $Å^{-1}$, respectively (i.e. on the FSDP in the liquid). Until *ca.* 0.8 ns, both structure factors are growing in intensity. At greater than 0.8 ns, the S(0–44) dies away and S(0–43) becomes even brighter. Beyond *ca.* 1.25 ns, the intensity of S(0–43) levels off with a magnitude indicating that around two-thirds of the cations are contributing. It is clear from figure 3 that the void structure will order in a manner mirroring the cation density (as observed in the liquid; see Wilson & Madden (1998)). Figure 5 shows the evolution of the coarse-grained void centres, allowing a clearer interpretation of the change in structure factor intensity with time. In the early stages of nucleation, the nucleus itself appears little affected by the presence of mirror images in neighbouring cells in the periodic system. At *ca.* 0.8 ns, the layers extend through the cell, and so the growing crystal changes its orientation as the initial direction of growth leads to a significant lattice mismatch perpendicular to the layers at the cell edges. The pseudo-two-dimensional nature of the layered crystal is such that the surface energies associated with cleavage perpendicular to the layers are typically ionic (of the order of joules per metre squared), while those involving the formation of surfaces parallel to the layers have typical molecular energies (of the order of millijoules per metre squared) (Israelachvili 1992). To attempt to eliminate the high boundary energy associated with the formation of the mismatched boundary, the layers glide over each other at *ca.* 0.8 ns, with an associated rotation of *ca.* 8°. The result is a crystal in which the layer mismatch is virtually eliminated, corresponding to a Bragg peak in the cation (void) density in the 0–43 direction.

The picture of nucleation that emerges from this study very much fits in with the picture of the behaviour in the liquid at higher temperatures (Wilson & Madden

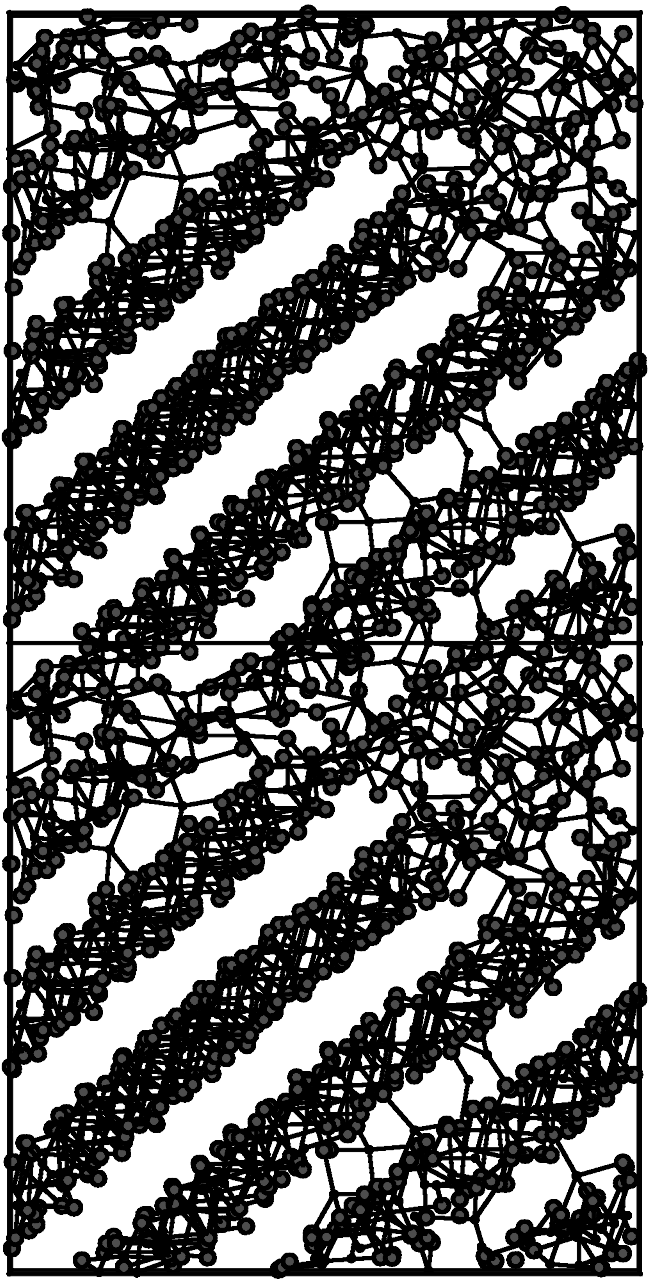

Figure 3. A molecular graphics 'snapshot' showing the formation of the layered crystal structure in the $ZnCl_2$ PIM at 600 K after *ca.* 1.5 ns of dynamics. Two neighbouring cells are shown to highlight the importance of the boundary in determining the crystal orientation.

1998), in which the regions are anisotropic, having transient layer-like structure. At 700 K, the typical residence times for these structures is *ca.* 40 ps, increasing to *ca.* 100 ps at 650 K. The increased residence times with decreasing temperature are

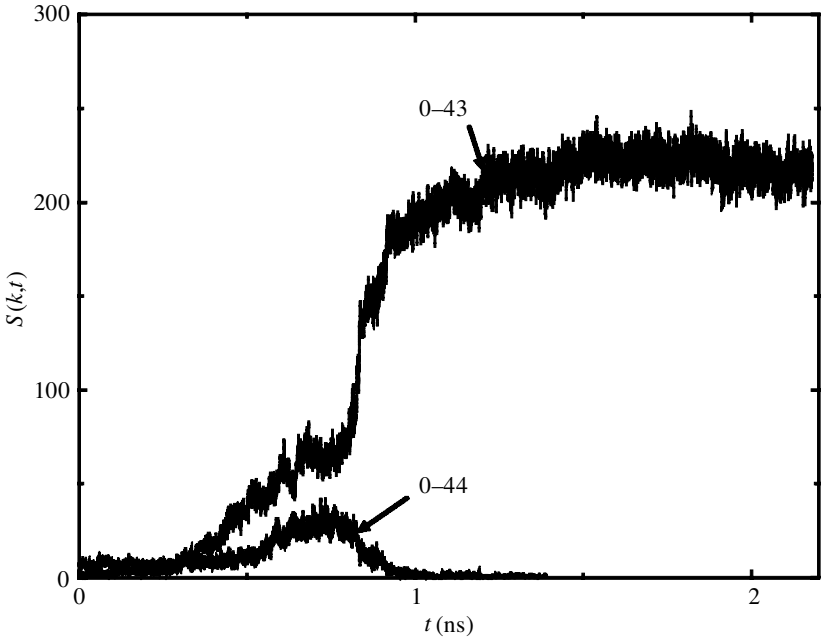

Figure 4. The evolution of two specific structure factors corresponding to the formation of the layered structure in the previous figure (see text for details).

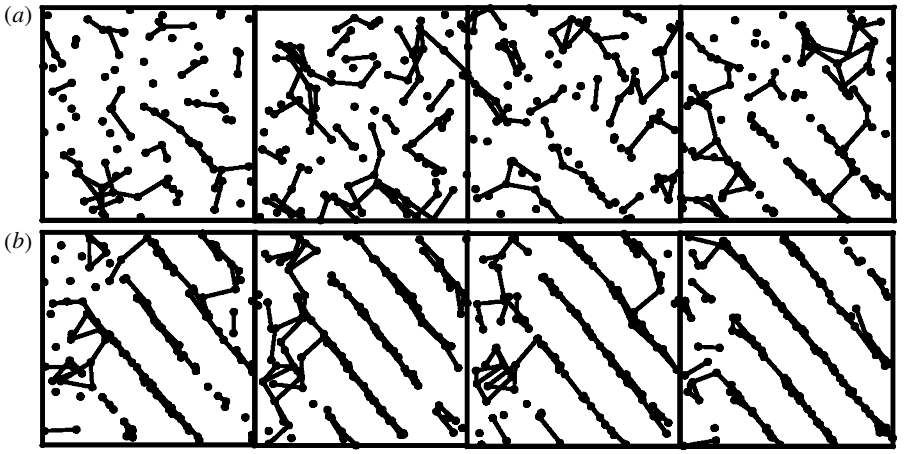

Figure 5. The evolution of the crystal nucleus as seen in the coarse-grained void structure. From left to right (*a*): after 120 ps, 240 ps, 360 ps and 600 ps. From left to right (*b*): after 840 ps, 1020 ps, 1200 ps and 1380 ps.

accompanied by an increase in the size of these regions. This picture fits well into a classical nucleation theory. At 650 K, the size of the anisotropic transient layered regions (the potential crystal nuclei) is not large enough to mount the activation barrier associated with crystallization. As the temperature is lowered to 600 K, however, the nuclei increase to beyond the critical size and so mount the activation barrier to crystallization.

Table 1. M–O *bond lengths in the annealed crystal at the equilibrium volume compared with experiment*

	(Li^+ in Si^{4+} layer)			(Li^+ in Al^{3+} layer)	
ion pair	R (AU)	r^{ai} (AU)[a]	r^{exp} (AU)[b]	r (AU)	r^{ai} (AU)
LiO	3.774, 3.764	3.746	3.711, 3.812, 3.932	3.780, 3.803, 3.837	3.778, 3.794
AlO	3.287	3.290	3.274	3.270	3.280
SiO	3.055	3.065	3.056	3.074	3.078

[a] Superscript 'ai' denotes *ab initio* calculations.
[b] From Pillars & Peacor (1973).

(*d*) *Complex systems*

As an example of a more complex system (a four-species model), we shall consider β-eucryptite, $LiAlSiO_4$. If a model can be constructed using the transferable potentials (i.e. from SiO_2, Al_2O_3 and Li_2O), it opens up the whole world of systems based on an oxide-linked Al^{3+} and Si^{4+} system, such as zeolites, many of which are important in catalysis (Catlow 1992). β-eucryptite itself is a useful ceramic, which has an unusual negative thermal expansivity along one crystal axis. Its crystal structure is based on that of α-quartz, in which the Al^{3+} and Si^{4+} cations sit alternately along the c-direction. The larger Li^+ ions sit in the large channels present in the c-direction.

In terms of the static structure, the pair-potential alone (i.e in the absence of polarization effects) tends to overestimate the length of the c-axis in the unit cell. Polarization effects lead to a slight *underestimation* of the c/a cell length ratio via the lowering of the Al–O–Si bond angle.

The fully relaxed unit cell gives an equilibrium a_0 of 5.33 Å ($ca.\,1.018 \times a_0^{exp}$) and a c_0 of 11.18 Å ($ca.\,1.0 \times c_0^{exp}$). Table 1 lists the equilibrium bond lengths for the three metal–anion ion pairs compared with the *ab initio* calculations (A. Lichtenstein, 1997, unpublished work) and experimental values at 23 °C (Pillars & Peacor 1973). Two types of Li^+ occupied site are considered in which the Li^+ cations occupy sites in the large channels of the quartz superstructure parallel to the Si^{4+} layers and Al^{3+} layers, respectively. The agreement between the model, *ab initio* calculations and experiment is very good.

Figure 6 shows the effect of moving the Li ions only along the large channels in the AlSiO superstructure in the c-direction. Two types of motion are considered in which all three Li^+ ions move cooperatively (Li_3), and in which just a single Li^+ ion moves (Li_1). An Li displacement of 0 indicates that the ion is sitting in the perfect site parallel to the Si^{4+} layer, and a displacement of 0.5 indicates that the Li ion is sitting in the Al^{3+} layer. The figure shows the relative energetics of these two modes for the relaxed and unrelaxed models and the *ab initio* calculations (an example of the use of indirect calculations). For both the relaxed and unrelaxed models, the barrier height associated with the motion of the Li_3 units through the oxide layers is underestimated by *ca.* 20% with respect to the *ab initio* calculations. More seriously, the fully relaxed model predicts that the occupation of the Al^{3+} layer site by the Li^+ ion will be energetically favourable over the occupation of the Si^{4+} layer site, in contrast to the *ab initio* calculations.

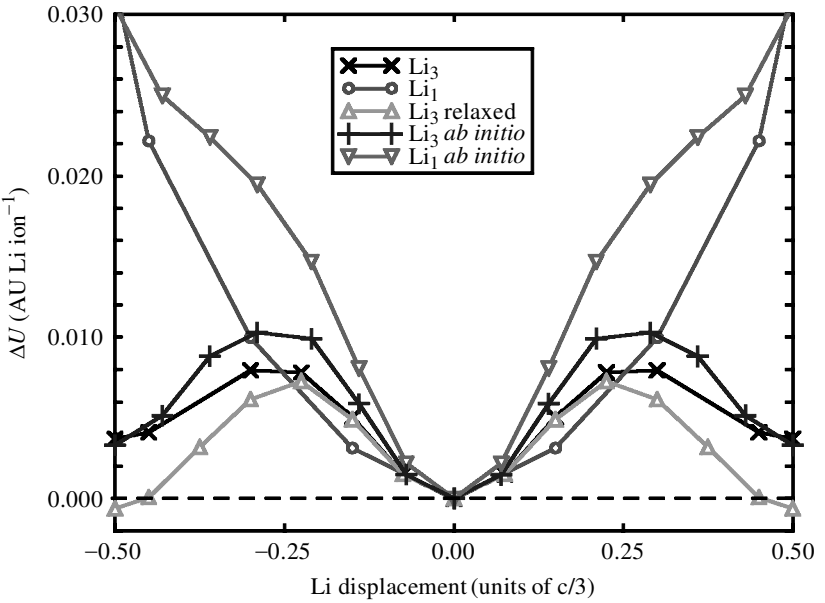

Figure 6. The effect of moving the Li^+ ions along the large channels in the crystal along the *c*-direction compared with independent *ab initio* calculations (A. Lichtenstein, 1997, unpublished work). The 1 and 3 subscripts refer to the effect of moving a single Li^+ against moving all three in the unit cell (effectively moving an infinite chain).

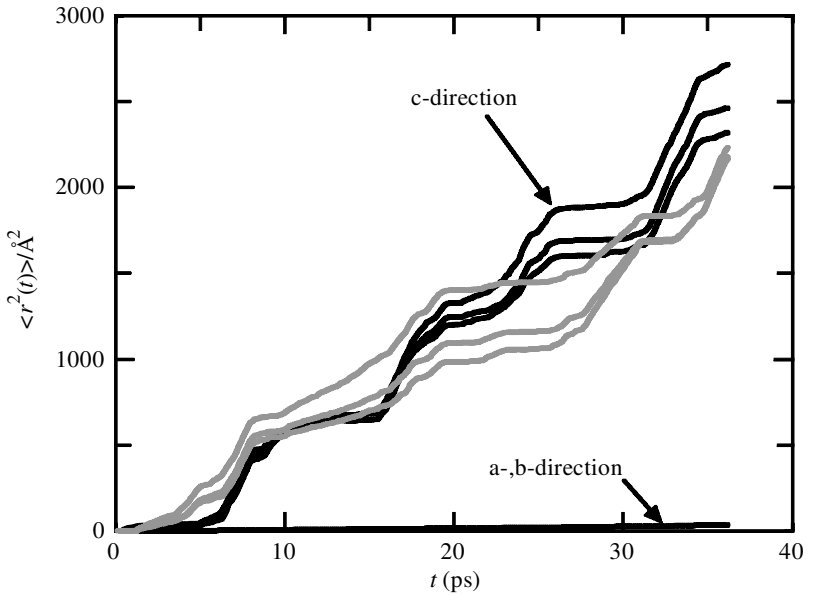

Figure 7. The mean-squared displacement for Li^+ ions in two different channels for a simulation of $LiAlSiO_4$ at 957 K. The three dark lines and three light lines correspond to the two sets of Li^+ ions in different channels, clearly showing the heavily correlated motion.

Table 2. *Raman frequencies calculated from the velocity autocorrelation functions compared with experiment*

mode	experiment (Mazza *et al.* 1993)	PIM
Si–O–Al asymmetric stretch	1160, 1050, 995	1092
Si–O–Al symmetric stretch	744, 673, 657	719
Li–O_4 stretch	520	514, 371, 273
Si–O–Al bend	470, 405	515

Molecular dynamics runs at 923 K and 757 K demonstrate the interesting dynamical behaviour of this system. Figure 7 shows the mean-squared displacement of six selected lithium ions in two different channels in the SiAlO superstructure. From figure 7, the following points are clear.

(i) The lithium ions are diffusing in the *c*-direction only, along the large channels clear in the SiAlO superstructure. The integrity of the AlSiO superstructure remains intact at these relatively low temperatures.

(ii) The diffusive motion of ions in the same channel is highly correlated, consistent with figure 6. Moving a single Li^+ brings the ion into relatively close contact with its *c*-direction Li^+ neighbour, leading to large coulombic repulsive interactions, which act to push the second ion in the same direction as the first.

(iii) The diffusive motion of the lithium ions is very 'jumpy': the ions seem to diffuse essentially by hopping between available sites in the SiAlO superstructure. Again, this behaviour is exactly what one would expect from figure 6, which indicates that the Li^+ ions encounter a series of activation barriers on moving in the *c*-direction. The thermal motion of the AlSiO superstructure, coupled with the cooperative nature of the Li^+ motion, will act to effectively randomize these barrier heights, leading to the hopping mechanism.

An important point of contact with experiment is via the Raman and IR spectra (Mazza *et al.* 1993). Table 2 lists the frequencies of the modes of vibration calculated from the Fourier transform of the velocity autocorrelation functions.

4. The future of computer models

Attempting to outline a view of the future in any field is highly problematic. Considering the field of computer simulation specifically, it is clear that both accessible time-scales and length-scales must increase. Additionally, the gap between *ab initio* and model calculations must close, leading to an increasingly symbiotic relationship in which high-level calculations are not only used to construct models but are actually embedded in them.

(*a*) *The role of simple models*

An increase in computer power, naturally enough, leads to an increase in the size of the *ab initio* calculation possible. However, it may be naive to assume that

such calculations will take over from those based on simple pairwise additive forces, as the same increase in power leads to larger possible simple calculations. As a result, whole classes of calculations, currently the domain of longer-range simulation methods and which are presently beyond the reach of atomistic models, may become practicable. Examples include the simulation of low-index grain boundaries, complex crystal growth, crack formation and nano-material properties.

The increase in time-scales allows for the bridge between experimental and simulation scales to be closed. In the study of the relaxation of systems on cooling, for example, the slowest rates accessible to simulation are still many orders of magnitude faster than those possible experimentally. Such problems have traditionally hindered the simulation of glass properties. In order to consider such systems, workers have been forced to attempt to circumvent the cooling problems by, for example, studying the liquid at just above the glass transition and then extrapolating to lower temperature, or by accepting the unphysical extreme cooling rates. These problems are particularly acute as the glass properties are known to be very dependent upon the precise sample history. As a result, the study of complex fibre-optic materials is currently problematic.

The idea that potential models for relatively complex systems can be constructed directly from those models for the simpler systems, here highlighted for $LiAlSiO_4$, is a non-trivial and important one. Traditionally, potential models have been relatively untransferable in this context. This has rendered the study of many-species systems very difficult as it is very difficult to parametrize the model at the most basic level. The ability to model such systems should lead to a great increase in the *predictive* properties of such models. At present, simulation models tend to lag behind both experiment and technologically important material developments. In the future, however, one would imagine that proven reliable models could be used to predict properties with great accuracy, and, therefore, take the lead over the more empirical methods employed at present.

(*b*) *The role of ab initio calculations*

The most obvious short-term route for *ab initio* calculations is to be able to fill in the gaps present in our present studies. For example, systems with heavy cation/anion combinations should become possible to the highest level of calculation. As a result, there will be an increase in the symbiotic relationship between the models and the *ab initio* calculations, with larger calculations specifically designed to focus on properties of interest leading to more accurate and, therefore, transferable models.

Such a procedure is, of course, not a unique combination of model and *ab initio* calculations. An alternative (and complementary) procedure is to embed a high-level *ab initio* calculation within a simpler model. Such a technique combines the advantages of *ab initio* calculations (chemical bond formation, charge transfer, etc.) with the length-scales possible with simpler models. Despite the considerable theoretical problems to overcome in making these models relatively simple to construct, it is clear that such techniques may allow the study of real chemical reactions currently beyond our capabilities. Such simulations will have a significant impact on, for example, the study of catalytic activity on surfaces.

(c) Visualization

The parallel increase in time- and length-scales presents non-trivial problems in terms of interpreting the system behaviour. Current simulations, in which systems of the order of 1000 particles are practicable, are *relatively* simple to understand, for example, displaying the particle coordinates. For larger systems, the human brain will be unable to take in the information. In the extreme (very distant future) limit, in which moles of atoms can be simulated, the analysis of the simulation itself evolves very much into the analogue of the actual experiments. As a result, the near future must bring an increase in visualization procedures focusing on the ways in which information may be reduced in order to access the important inherent system properties.

The author is indebted to Paul Madden for many years of useful discussions. He also thanks Patrick Fowler and Patrick Ӧemmer for collaborations incorporating many of the *ab initio* calculations, and Dr A. I. Lichtenstein for providing the *ab initio* calculations on β-eucryptite. The author also thanks The Royal Society for a Research Fellowship.

References

Allen, M. P. & Tildesley, D. J. 1987 *Computer simulation of liquids*. Oxford: Clarendon.
Allen, M. P. & Tildesley, D. J. (eds) 1993 *Computer simulation in chemical physics*. Kluwer.
Bernal, J. D. 1964 *Proc. R. Soc. Lond.* A **280**, 299.
Boyer, L. L., Mehl, M. J., Feldman, J. L., Hardy, J. R., Flocken, J. W. & Fong, C. Y. 1985 *Phys. Rev. Lett.* **54**, 1940.
Car, R. & Parrinello, M. 1985 *Phys. Rev. Lett.* **55**, 2471.
Catlow, C. R. A. (ed.) 1992 *Modelling of structure and reactivity in zeolites*. Academic.
Dick, B. G. & Overhauser, A. W. 1958 *Phys. Rev.* **112**, 90.
Domene, C., Fowler, P. W., Ӧemmer, P. & Madden, P. A. 1999 *Chem. Phys. Lett.* **299**, 51.
Elliott, S. R. 1990 *The physics of amorphous materials*, 2nd edn. London: Longmans Green.
Elliott, S. R. 1991 *Nature* **354**, 451.
Enderby, J. E. & Barnes, A. C. 1990 *Rep. Prog. Phys.* **53**, 85.
Finney, J. L. 1970 *Proc. R. Soc. Lond.* A **319**, 495.
Fowler, P. W. & Madden, P. A. 1985 *Phys. Rev.* B **31**, 5443.
Gale, J. D., Catlow, C. R. A. & Mackrodt, W. C. 1992 *Modelling Simul. Mater. Sci. Engng* **1**, 73.
Harding, J. H. 1990 *Mol. Sim.* **4**, 255.
Harding, J. H. & Pyper, N. C. 1995 *Phil. Mag. Lett.* **71**, 113.
Israelachvili, J. 1992 *Intermolecular and surface forces*. Academic.
Ӧemmer, P., Fowler, P. A., Wilson, M. & Madden, P. A. 1998 *J. Phys. Chem.* A **102**, 8377.
Ӧemmer, P., Wilson, M., Fowler, P. W. & Madden, P. A. 1999 *J. Chem. Phys.* **111**, 2038.
Kumta, P. N., Deymier, P. A. & Risbud, S. H. 1988 *Physica* B **153**, 85.
Lacks, D. J. & Gordon, R. G. 1993 *J. Geophys. Res.* **98**, 22 147.
Lewis, G. V. & Catlow, C. R. A. 1985 *J. Phys. C: Solid State* **18**, 1149.
Madden, P. A. & Wilson, M. 1996 *Chem. Soc. Rev.* **25**, 339.
Mahan, G. D. & Subbaswamy, K. R. 1990 *Local density theory of polarizability*. London: Plenum.
Mazza, D., Lucco-Borlera, M., Busca, G. & Delmastro, A. 1993 *J. Eur. Ceram. Soc.* **11**, 299.
Naberukhin, Y. I., Voloshin, V. P. & Medvedev, N. N. 1991 *Molec. Phys.* **73**, 917.
Pillars, W. W. & Peacor, D. R. 1973 *Am. Miner.* **58**, 681.
Pyper, N. C. 1991 *Adv. Solid State Chem.* **2**, 223.

Rowley, A. J., Jemmer, P., Wilson, M. & Madden, P. A. 1998 *J. Chem. Phys.* **108**, 10 209.
Rowley, A. J., Wilson, M. & Madden, P. A. 1999 *J. Phys. Condensed Matter* **11**, 1903.
Sangster, M. J. L. & Dixon, M. 1976 *Adv. Phys* **23**, 247–342.
Schröder, U. 1966 *Solid State Commun.* **4**, 347.
Sprik, M. 1991*a* *J. Phys. Chem.* **95**, 2283.
Sprik, M. 1991*b* *J. Chem. Phys.* **95**, 6762.
Sprik, M. & Klein, M. L. 1988 *J. Chem. Phys.* **89**, 7556.
Sprik, M., Klein, M. L. & Watanabe, K. 1990 *J. Phys. Chem.* **94**, 6483.
Tang, K. T. & Toennies, J. P. 1984 *J. Chem. Phys.* **80**, 3726.
Vashishta, P., Kalia, R. K., Rino, J. P. & Ebbsjö, I. 1990 *Phys. Rev.* B **41**, 12 197.
Wilson, M. & Madden, P. A. 1997*a* *Molec. Phys.* **90**, 75.
Wilson, M. & Madden, P. A. 1997*b* *J. Chem. Soc. Faraday Trans.* **106**, 339.
Wilson, M. & Madden, P. A. 1998 *Phys. Rev. Lett.* **80**, 532.
Wilson, M., Costa-Cabral, B. J. & Madden, P. A. 1996*a* *J. Phys. Chem.* **100**, 1227.
Wilson, M., Huang, Y.-M., Exner, M. & Finnis, M. W. 1996*b* *Phys. Rev.* B **54**, 15 683.
Wilson, M., Madden, P. A., Pyper, N. C. & Harding, J. H. 1996*c* *J. Chem. Phys.* **104**, 8068.
Woodcock, L. V. & Singer, K. 1971 *Trans. Faraday Soc.* **67**, 12.
Woodcock, L. V., Angell, C. A. & Cheeseman, P. 1976 *J. Chem. Phys.* **65**, 1565.

AUTHOR PROFILE

M. Wilson

Mark Wilson was born in Derby in 1968. He obtained his BA in chemistry with first class honours from Keble College, Oxford, in 1991 and his DPhil in 1994. He was then awarded an Alexander von Humboldt Fellowship, which he took up at the Max-Planck Institut für Werkstoffwissenschaft in Stuttgart. At the present time he is a Royal Society Research Fellow in the Physical and Theoretical Chemistry Laboratory at Oxford. His scientific interests centre around the construction and use of computer simulation models to study problems over a range of length- and time-scales. He has published around 40 papers in this area.

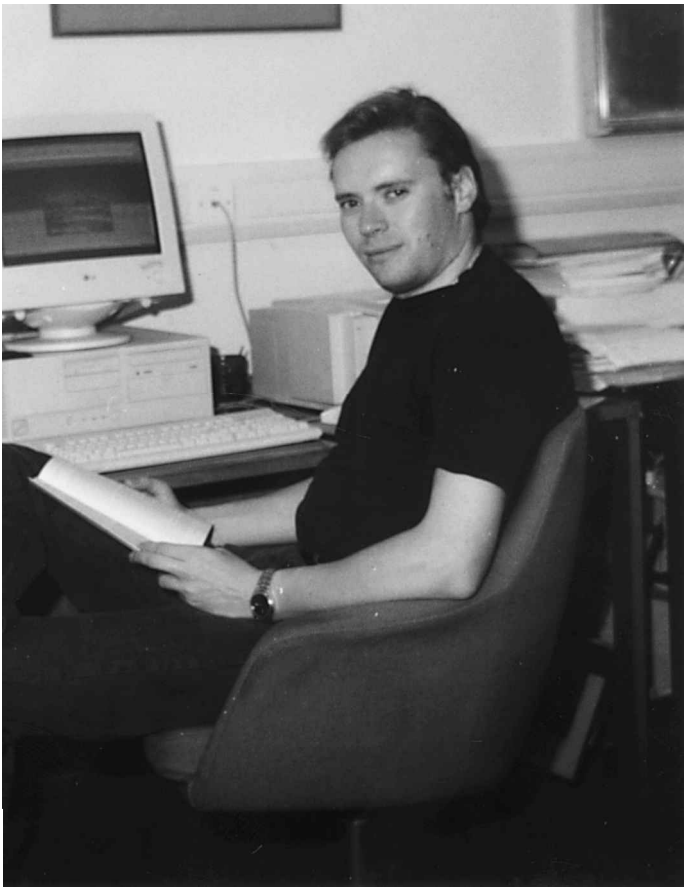

PHILOSOPHICAL TRANSACTIONS OF THE ROYAL SOCIETY A MATHEMATICAL, PHYSICAL & ENGINEERING SCIENCES